Chapter 3

Base Mediated Anaerobic Oxidation of Benzyl Alcohols over Reusable MOP-Am2

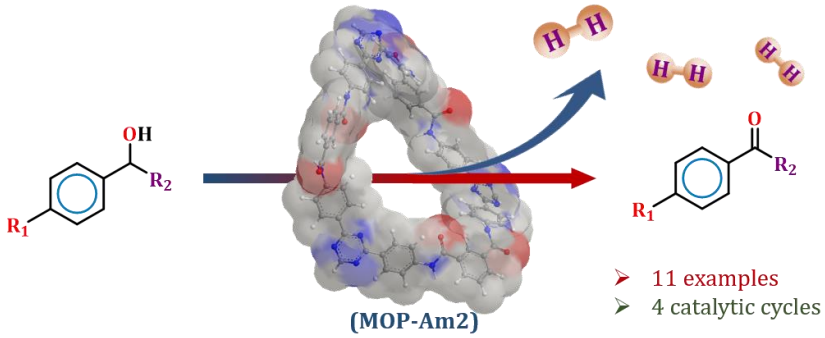

3.1 Introduction

The selective oxidation of benzyl alcohols to the corresponding benzaldehydes is one of the most fundamental oxidation reactions gaining attention owing to its wide applications in the field of chemical and pharmaceutical industries. In addition, it is commonly utilized as an intermediate for the manufacture of medicine, colorants, and agrochemicals [1-4]. Traditional commercial method includes the hydrolysis of benzyl chloride. But the process includes the release of highly poisonous chlorine gas. Classically such oxidative processes were carried out by employing Corey's Reagent, Swern oxidation, Dess-Martin Reaction etc. which are not environment friendly [5-7]. The process also leads to the formation of over oxidized product viz. carboxylic acid. So, the selective oxidation of benzyl alcohols to benzaldehyde with environmentally benign method is imperative. Literature reveals the use of precious metals (such as Au, Pd, Ru, Pt) supported species as catalyst with oxidants being H_2O_2, expensive *tert*-butylhydroperoxide (TBHP) and in few cases O_2 [8-13].

A. Au-Pd supported on TiO_2 catalysed benzyl alcohol oxidation with H_2O_2 [9].

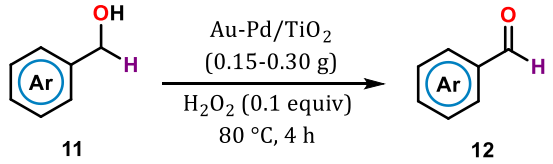

11 12

B. Pt-supported on Carbon Hybrids catalysed benzyl alcohol oxidation with O_2 [12].

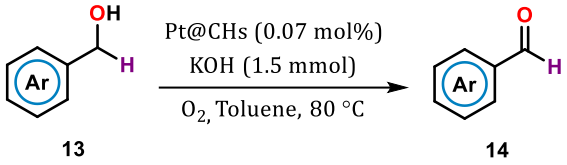

13 14

C. Ru-catalysed primary alcohol oxidation with O_2 [13].

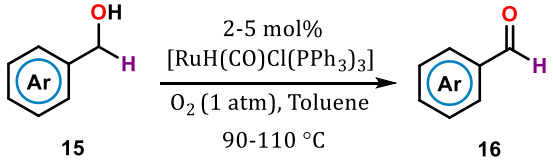

15 16

These metal catalysts have vacant coordination sites, providing opportunities for water molecules to coordinate. As a consequence, it neutralizes the performance of such metals towards oxidation process and leftover as toxic traces of heavy metals in the product. Thus, it is needless to mention that developing environmentally

friendly new oxidization protocol is highly desirable. Recently MOF with Cu, Fe, Co and Ru as central metal atoms have been used for aerobic oxidation of benzyl alcohol with high selectivity [14,15]. Gold nanoparticle encapsulated MOF notably Au/UiO-66 has been reported as a green catalyst for solvent free oxidation of benzyl alcohol under atmospheric pressure [1]. The importance of *in-situ* palladium nanoparticle formation has also been explored in benzyl alcohol oxidation on ferrocene-based MOF [16].

Further investigations, however not so far, reveal the use of porous organic polymer as organocatalyst for such oxidation reaction. Hu and coworkers demonstrated the combination of polyoxometalate catalyst with a porous covalent triazine framework ($PMo_{10}V_2$@CTF) exhibits remarkable activity for the selective electrocatalytic oxidation of alcohols to aldehydes achieving 99% conversion [17].

D. $PMo_{10}V_2$@CTF electrocatalysed benzyl alcohol oxidation [17].

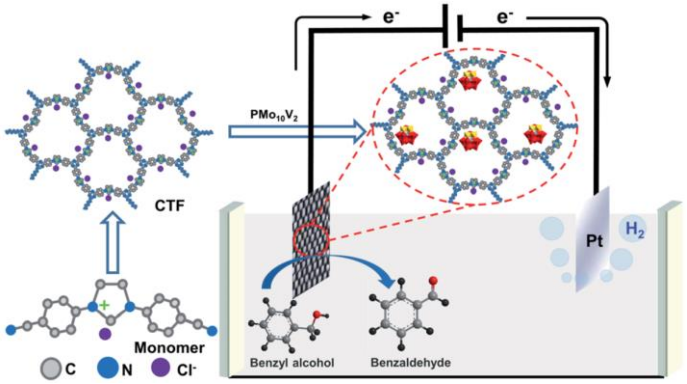

E. Carbazole scaffold containg H-CTB CMPs photocatalysed benzyl alcohol oxidation [18].

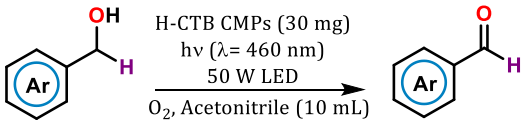

17 18

Other known catalytic pathways for such conversion comprised POPs based on carbazole or heptazine moiety that reacted under photocatalytic conditions in an atmospheric oxygen [18,19]. These findings stimulate the development of a metalfree protocol for selective benzyl alcohol oxidation in order to achieve an ecologically friendly catalytic route. Herein we have exploited the designed MOP-Am2, established in chapter 2, as a facilitator for the controlled oxidation of benzyl alcohol under basic media.

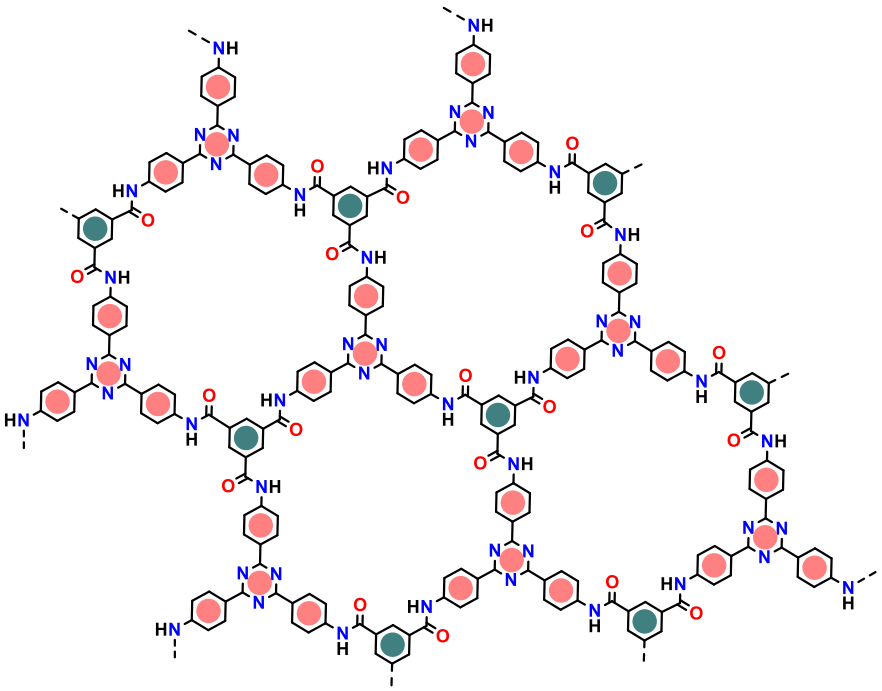

Figure 3.1 Schematic representation of the structural architecture of MOP-Am2

Investigation suggested that inclusion of heteroatom in the backbone of the POP network led to structural defects which enhances the catalytic activity by modulating multiple active sites [20]. The triazine moiety present in MOP-Am2 has changed the overall catalytic pathway following a hydride elimination mechanism which permitted to avoid any metal source or external oxidant for the catalytic transformation, hence making it as environmentally benign strategy.

This work

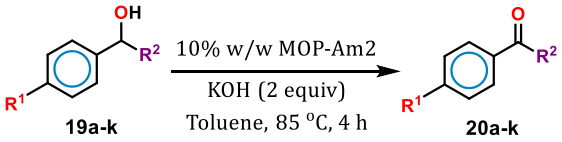

Scheme 3.1 MOP-Am2 catalysed anaerobic oxidation of benzyl alcohols

3.2 Results and Discussion

3.2.1 Catalytic oxidation of benzyl alcohol

Benzyl alcohol oxidation to benzaldehyde selectively has been often considered as a benchmark reaction to evaluate the catalytic activity of porous polymers. We have extended our study to assess MOP-Am2's activity in the oxidation of benzyl alcohols to corresponding aldehydes, which usually demand metal catalyst and oxidant such as H_2O_2, TBHP or O_2 etc [11-13,21]. It is worth mentioning that the MOP-Am2's

performance as a metal free catalyst for the selective oxidation of benzyl alcohols to the corresponding benzaldehydes was effective with no added oxidant (Scheme 3.1). The reaction was believed to be initiated and progressed by base in presence of MOP-Am2. This was supported by the preliminary observation of the reaction progress being gathered from TLC analysis. Recent reports demonstrated analogous catalytic function of π-conjugated amide linked 2D organic polymer in such transformation reaction [22]. The reaction follows a free radical pathway with *tert*-butylhydroperoxide (TBHP) as oxidant. Perhaps, this reaction debarred from the use of any oxidant and/or peroxide or O_2 as oxidizing agent. Rather, the environment friendly oxidation was initially carried out in presence of KOH. Only few reports uncover such oxidation of benzyl alcohols assisted by KOH while illustrating the formation of imine substrates through *in-situ* benzaldehyde as intermediates [23]. Trapping of the aldehyde intermediates, biologically an important precursor, selectively which otherwise are obtained from the oxidation of benzyl alcohols deploying precious and expensive metal catalyst marks the sagacity in organic synthesis.

The optimal reaction condition for this oxidation reaction was achieved after the trial with several physical and chemical factors listed in Table 3.1. To understand the necessity of the catalyst behind these transformations, we have cross-checked the reactions with individual KOH and MOP-Am2 separately under all the other reaction conditions identical. But the reaction does not proceed to a significant extent. Upon the addition of MOP-Am2 in catalytic amount (10 wt% with respect to **19**) to the solution of benzyl alcohol and KOH, the reaction proceeds with a good-to-better yield of aldehydes without over-oxidation or any side product formation. Playing with various physical and chemical parameters, such as solvents, base, catalyst amount, temperature and time, the best result obtained in toluene as solvent in presence of MOP-Am2 mediated by KOH (Table 3.1, entry 15). While the reaction showed no progress without the catalyst and base (Table 3.1, entry 1 & 7) which clearly suggested that MOP-Am2 and the base were the essential condition in the reaction. Formation of the product was confirmed by performing the GCMS analysis. The reaction proceeds successfully under anaerobic conditions, yielding benzaldehydes with 100% selectivity.

Table 3.1 Reaction condition optimization for the catalytic oxidation of benzyl alcohol taking 4-methylbenzyl alcohol as the initial substrate[a]

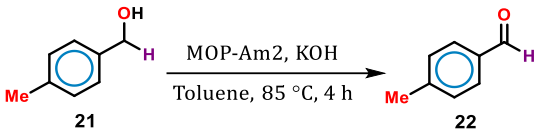

Entry	MOP-Am2 wt%	Solvent (mL)	Base (Equiv)	Temperature (°C)	Time (h)	**22** % Yield[b]
1	-	Toluene	KOH (3)	100	6	NR
2	5	Toluene	KOH (3)	100	6	42
3	10	Toluene	KOH (3)	100	6	64
4	15	Toluene	KOH (3)	100	6	65
5	10	CH_3CN	KOH (3)	100	6	NR
6	10	H_2O	KOH (3)	100	6	NR
7	10	Toluene	-	100	6	NR
8	10	Toluene	NaOH (3)	100	6	35
9	10	Toluene	K_2CO_3 (3)	100	6	NR
10	10	Toluene	KOH (2)	100	6	65
11	10	Toluene	KOH (1)	100	6	28
12	10	Toluene	KOH (2)	90	6	65
13	10	Toluene	KOH (2)	85	6	64
14	10	Toluene	KOH (2)	80	6	40
15	10	Toluene	KOH (2)	85	4	64
16	10	Toluene	KOH (2)	85	2	49

[a]Reaction conditions: **21** (0.5 mmol), Toluene (1 mL), MOP-Am2 (10 wt% of **21**), KOH (2 equiv), T (85 °C), time (4 h). [b]GC yield. NR: No reaction.

With the optimized reaction conditions, in order to generalize the protocol, the reaction was carried out with eleven varied substituted benzyl alcohols connected with electron-withdrawing and electron-donating groups and tabulated in Table 3.2. The product identification and their corresponding yields were determined by GC-MS analysis. The reaction resulted good conversion up to 69%.

Table 3.2 Substrate scope study for benzyl alcohol oxidation employing MOP-Am2 as catalyst mediated by KOH.[a][b]

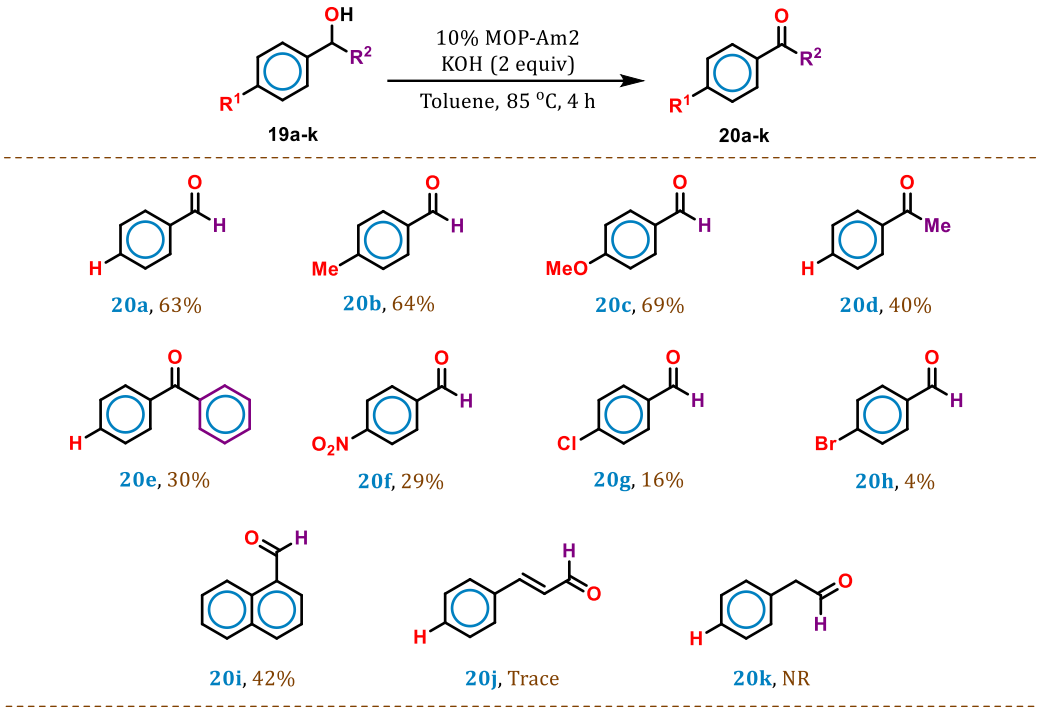

[a] Reaction conditions: **19a-k** (0.5 mmol), Toluene (1 mL), MOP-Am2 (10 wt% of benzyl alcohol), KOH (2 equiv), T (85 °C), time (4 h). [b] Product characterization and yields are confirmed by GC-MS analysis. NR: No reaction.

3.2.2 Mechanism study

3.2.2.1 Experimental approach

To understand the chemistry behind these transformations, we cross-checked the reactions with individual KOH and MOP-Am2 separately under identical conditions, but the reaction did not proceed (Table 3.1, entry 1 and entry 7). Upon the addition of MOP-Am2 in catalytic amount (10 wt% w. r. t. alcohols) to the solution of benzyl alcohol and KOH, the reaction proceeded with a good-to-better yield of aldehydes without over-oxidation or any byproduct formation (Table 3.1, entry 10). Reported studies validated the free-radical mechanism at large for such selectivity with peroxide or molecular oxygen as oxidizing agents [7]. In this context, a control experiment was carried out for this transformation reaction to establish the actual mechanistic pathway. The reaction was mimicked under a nitrogen atmosphere with the addition of 2,2,6,6-tetramethylpiperidinyl-1-oxy (TEMPO), a radical scavenger, to the reaction mixture. We were amazed to see that the reaction did not freeze,

which ruled out the generation of free radicals in the reaction mixture (Table 3.3, equation (i)). Moreover, the oxidation reaction was successful under anaerobic conditions too, and the probable involvement of molecular oxygen in the reaction is nullified (Table 3.3, equation (ii)). Understanding the role of catalyst in catalytic reactions is an imperative factor, and for that identical oxidation reactions have been performed employing other nitrogenous compounds, viz., aniline and triethylamine (Et_3N) in lieu of MOP-Am2. Interestingly, the oxidation of benzyl alcohols occurred yielding the corresponding benzaldehydes selectively using Et_3N as the homogeneous catalyst (Table 3.3, equation (iii)). However, with aniline at a catalytic amount, the product formed was the corresponding imine compound via the *in-situ* generation of benzaldehyde (Table 3.3, equation (iv)). Thus, an intriguing fact could be drawn from this experiment, rendering the vital role of nitrogen atom present in the catalyst. Considering all the experimental factors that affect the oxidation of benzyl alcohol derivatives, the best plausible mechanism during this transformation can be agreed with the involvement of hydride ion elimination that reacts further with K^+ and H_2O to give H_2.

Table 3.3 Control experiment for the selective oxidation of benzyl alcohol to corresponding aldehyde.

i. Reaction with 2,2,6,6-tetramethylpiperidinyl-1-oxy (TEMPO)

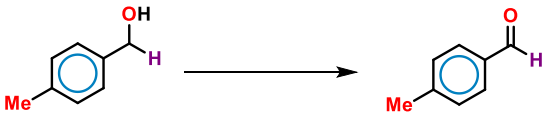

---------- (i)

ii. Reaction under innert condition (N_2 gas)

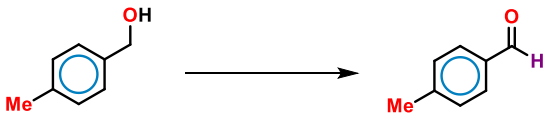

---------- (ii)

iii. Reaction with triethyl amine (Et_3N) and aniline

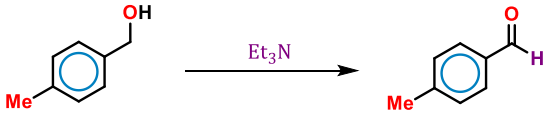

---------- (iii)

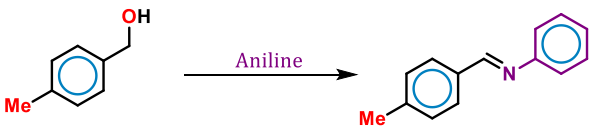

---------- (iv)

The aforesaid reaction was accomplished efficiently in presence of the polymer MOP-Am2. Indeed, using MOP-Am2 with available delocalized π-electronic cloud and

sufficient N atoms augment the catalytic progression with better oxidative conversion. To investigate the role of conjugated π-electrons available in MOP-Am2 in the catalytic oxidation of benzyl alcohol, we performed the oxidation process considering both the monomeric unit (MOP-Am2-m, discussed in chapter 2) and MOP-Am2 as catalyst. Reaction progression was confirmed by no catalyst no product condition. The oxidative conversion was reduced for genuine reasons with MOP-Am2-m as catalyst, but MOP-Am2 having available delocalized π-electronic cloud and enriched N atoms accelerated the conversion to a great extent. Figure 3.2 eventually conferred the performances will go better if the monomeric unit (MOP-Am2-m) extends the conjugation through their arms.

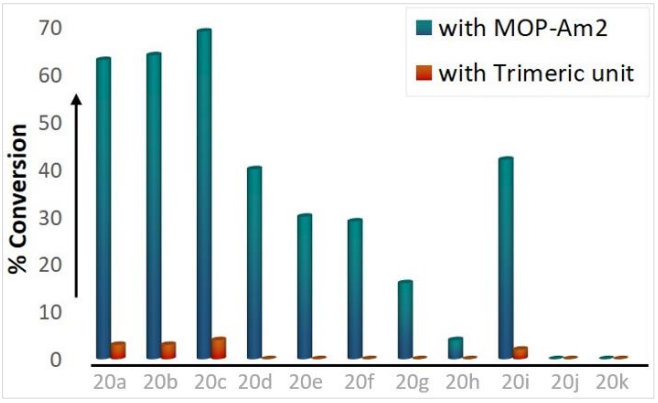

Figure 3.2 Comparative bar diagrams defining the percentage conversion of benzyl alcohol derivatives in presence of MOP-Am2 and MOP-Am2-m

3.2.2.2 Computational approach

With the limited competence it was difficult to carry a computational study on the catalytic behavior of the MOP-Am2. Since the monomeric unit, MOP-Am2-m is essentially an active catalyst for the reactions studied, we used the same in place of MOP-Am2 structure for calculation. The geometrical configuration of MOP-Am2-m and the incoming benzyl alcohol was optimized at BP86-D3BJ/6-311++G** level of theory without any symmetry constraints. To investigate the most probable site of interaction on MOP-Am2-m, the z-component of nucleus independent chemical shift ($NICS_{zz}$) values were calculated at 1Å above the plane of the rings. It is evident from Figure 3.3a that the central triazine ring is the most electron rich center with highest negative value of $NICS_{ZZ}(1)$ suggesting it to be the most appropriate site for the adsorption. Initially the benzyl alcohol adsorbed on the surface of MOP-Am2-m via

non-covalent interaction involving the O–H group of benzyl alcohol with the π cloud of the central ring of MOP-Am2-m. Figure 3.3b has shown the optimized geometry of the adsorbed benzyl alcohol on the surface of MOP-Am2-m. The distance between the H atom of the O–H group of benzyl alcohol and the center of the triazine ring is 3.037 Å. To investigate the possibility of non-covalent interaction, we have performed NCI analysis on the optimized geometry. The NCI plot in Figure 3.3c has shown the formation of O–H···π interaction. In addition, π···π interaction was also observed between the π cloud of the benzyl alcohol and the π-cloud of the aryl ring of MOP-Am2-m (Figure 3.3c). All these interactions suggested that the adsorption of benzyl alcohol on the surface of MOP-Am2-m was stabilized. The interaction energy was calculated to be 6.7 kcal/mol.

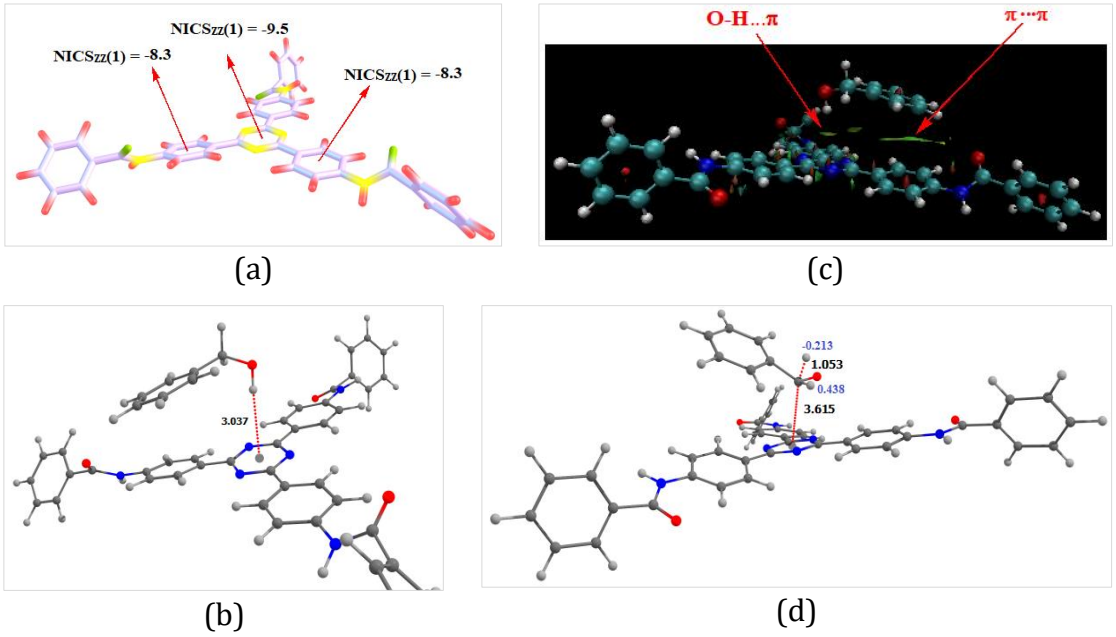

Figure 3.3 (a) $NICS_{ZZ}(1)$ plot (values in ppm) of monomeric unit, MOP-Am2-m. (b) Optimized geometry of MOP-Am2-m and incoming benzyl alcohol via weak non-covalent interaction. (c) NCI plot of benzyl alcohol on MOP-Am2-m. (d) Optimized geometry of $PhCH_2O^-$ on MOP-Am2-m via benzylic carbon. Bond length is in Å (black) and natural charge at the H atoms in blue

Investigating the molecular structure of the reactants and experimental evidences we ponder the reaction might proceed through the formation of corresponding phenoxide ion of benzyl alcohols in presence of KOH. The $PhCH_2O^-$ ion then bound to the MOP-Am2-m surface through the benzylic carbon atom. It is evident from Figure 3.3d that one of the H attached to the benzylic carbon atom bears a significant

negative charge (shown in blue colour) with an elongated C–H bond. This indicates that the hydride elimination would be a likely pathway.

With the experimental and computational results, it is confirmed that upon increasing the electron push ability on benzylic carbon, more will be the negative charge on benzylic proton, thus loosen the C–H bond. This fact stands for how the inductive effect hampers the yield. Subsequently the oxide aromatized to form relatively stable carbonyl compounds via elimination of hydride ion. Highly unstable and reactive hydride in presence of K^+ and water afforded KOH, with the elevation of H_2 gas, that reacted further; and the reaction continued. However, a competitive yield formation compared to 1-methylbenzyl alcohol, **20d** was found in case of diphenyl methanol with 30% yield, **20e**. This is due to the formation of stable conjugated benzophenone.

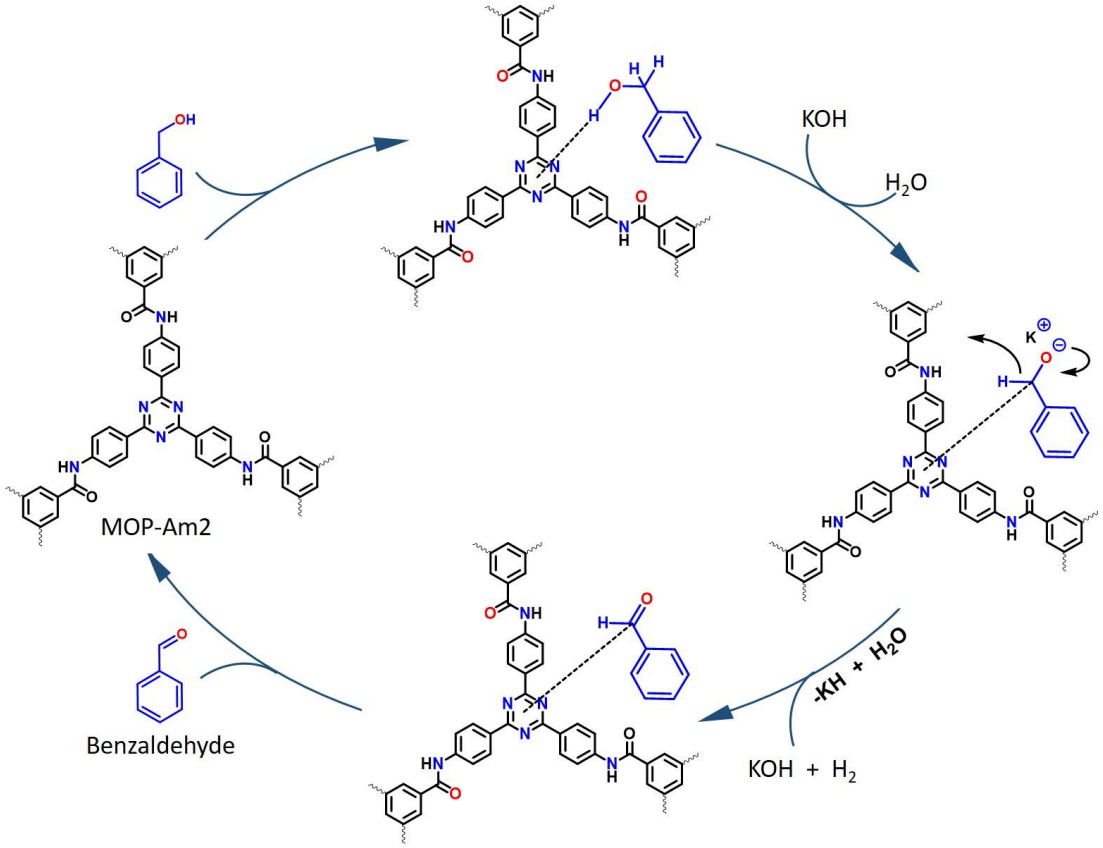

Figure 3.4 Plausible hydride eliminated mechanistic pathway during the formation of benzaldehyde from benzyl alcohol driven by KOH

On the other hand, when identical reaction condition applied on 2-phenylethanol, no product was formed, **20k**. This fact attributes because of the negative charge is now

localized on oxygen in presence of the base and thus loose aromaticity. This confirmed the π-conjugation to be the stabilizing factor for benzaldehyde formation. The product benzaldehyde is stabilized over the catalyst surface via π···π and C–H···π interactions, thereby precluding over-oxidation. From the computational data and experimental evidences, the best plausible mechanism for this anaerobic oxidation is established (Figure 3.4).

3.2.3 Detection of hydride elimination

To confirm the involvement of hydride elimination, we have tried to carry an *in-situ* reduction reaction of Diphenyl acetylene in presence of 10% palladium on activated charcoal (10% Pd/C) taking 4-Methylbenzyl alcohol as model system (Scheme 3.2).

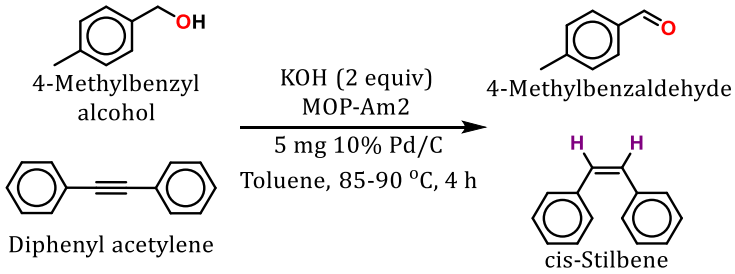

Scheme 3.2 *In-situ* reduction of Diphenyl acetylene accelerated by oxidation of 4-Methylbenzyl alcohol

Generation of a new singlet peak at 6.52 ppm in the ^{1}H NMR spectrum is assigned for the addition of H_2 to the acetylene (Figure 3.5) and the downfield shift of ^{13}C signal from 89.4 ppm to 130.4 ppm (Figure 3.6) are responsible for the reduction of sp to sp^2 hybridized carbon. The shifting of the signal responsible for the phenylic carbon attached to the acetylene in ^{13}C NMR spectrum from 123.3 ppm to 137.4 ppm also confirmed the formation of cis-stilbene (Figure 3.6).

Spectral analysis of *cis*-Stilbene:

^{1}H NMR (400 MHz, $CDCl_3$, 298 K) δ (ppm): 7.20-7.08 (m, 10H), 6.52 (s, 2H). $^{13}C\{^{1}H\}$ NMR (101 MHz, $CDCl_3$, 298 K) δ (ppm): 137.4, 130.4, 129.0, 128.4, 127.3.

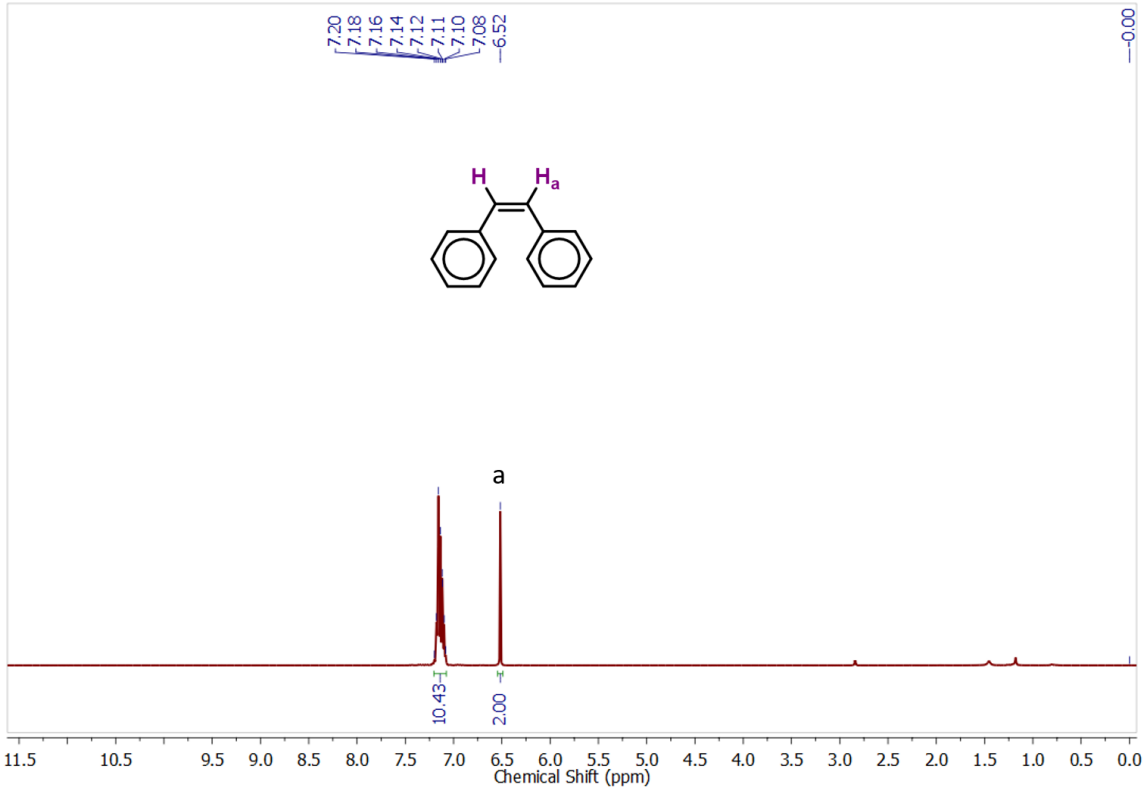

Figure 3.5 ^{1}H NMR ($CDCl_3$, 400 MHz, 298 K) of *cis*-Stilbene

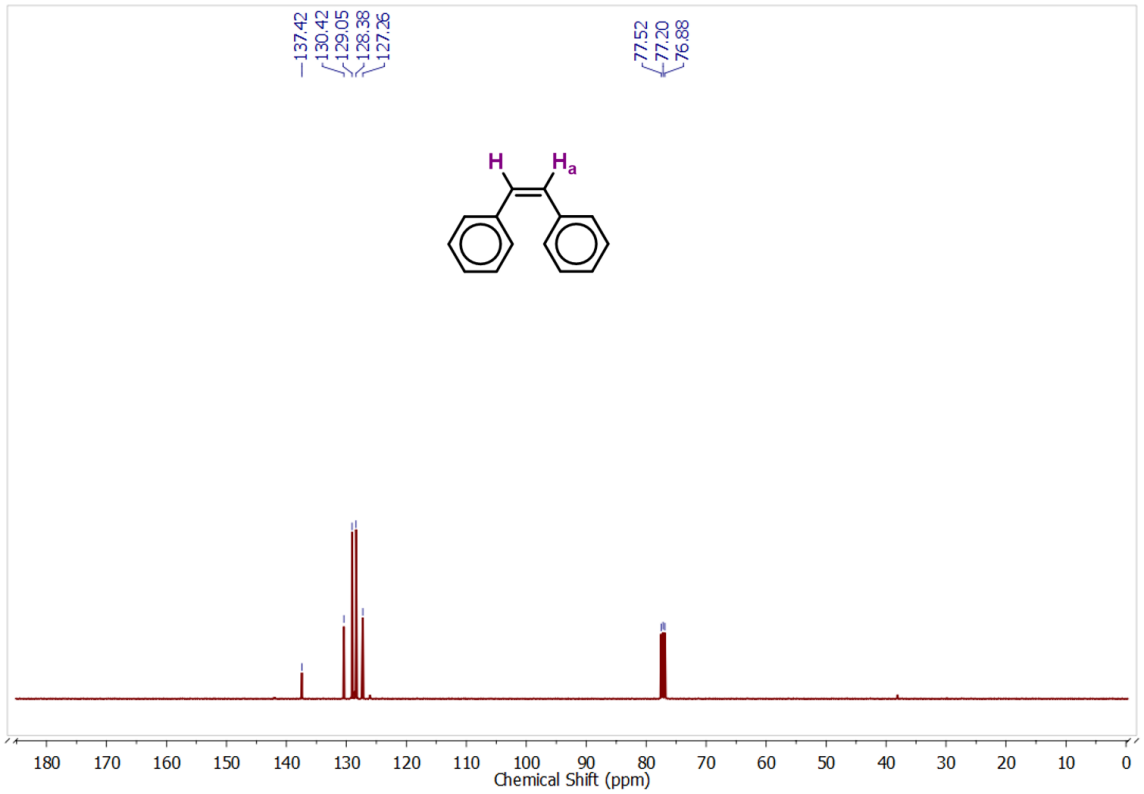

Figure 3.6 $^{13}C\{^{1}H\}$ NMR ($CDCl_3$, 101 MHz, 298 K) of *cis*-Stilbene

3.2.4 Role of the MOP-Am2 as catalyst

To comprehend the role of MOP-Am2 and its extended π-conjugation onto the reactions, we performed the same oxidation reaction under the optimum reaction conditions by adding only MOP-Am2-m as catalyst promoter. The reaction proceeded with low to nil conversion of starting materials into products. Thus, it indicates that MOP-Am2 having extended conjugation of delocalized π-electrons has an imperative role as catalyst (Figure 3.2). Reported study has already demonstrated how red-shift of band gap examined by electronic absorption spectroscopy influences the performance of the π-electronic functions of 2D extended ordered polymer [23].

It is affirmative to observe a decrease in band gape for MOP-Am2 when compared to its basic monomeric unit, MOP-Am2-m from 2.60 eV to 1.95 eV (Figure 3.7). This indeed enhances the probability for easy electronic transition that could promote catalysis. Thus, effective catalytic activity of MOP-Am2 is attributed to the rich delocalize conjugated π-electrons due to the presence of nitrogen heteroatom, leading to a strong π···π or C–H···π interaction between the catalyst and the benzyl alcohols [8,23-25]. In effect, it gears up the electron transfer process amongst the catalyst and the individual substrate and thereby stimulate catalysis.

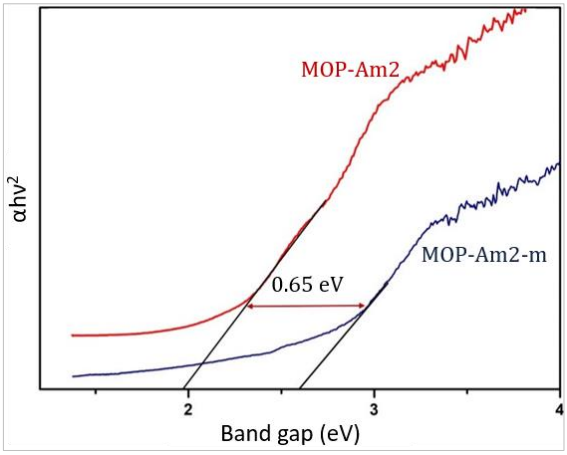

Figure 3.7 Tauc plot for MOP-Am2-m and MOP-Am2

3.2.5 Reusability and stability of MOP-Am2

To investigate the heterogenicity of the reaction, we performed the reusability test taking *4*-methoxybenzyl alcohol to its corresponding aldehyde, **20c** as the model reaction. Interestingly, the reusability and stability test indicate high efficiency of the

catalyst promoter up to 4th cycle for benzyl alcohol oxidation (Figure 3.8a). Since KOH is not completely soluble in toluene, thus few portions of KOH occupy the pores of MOP-Am2 continuously decreasing its activity and also it becomes difficult to wash it with water after few catalytic cycles due to its stickiness. However, the reused catalyst was characterized by FT-IR analysis (Figure 3.8b) and is found to be stable enough to utilize it again after complete removal of KOH.

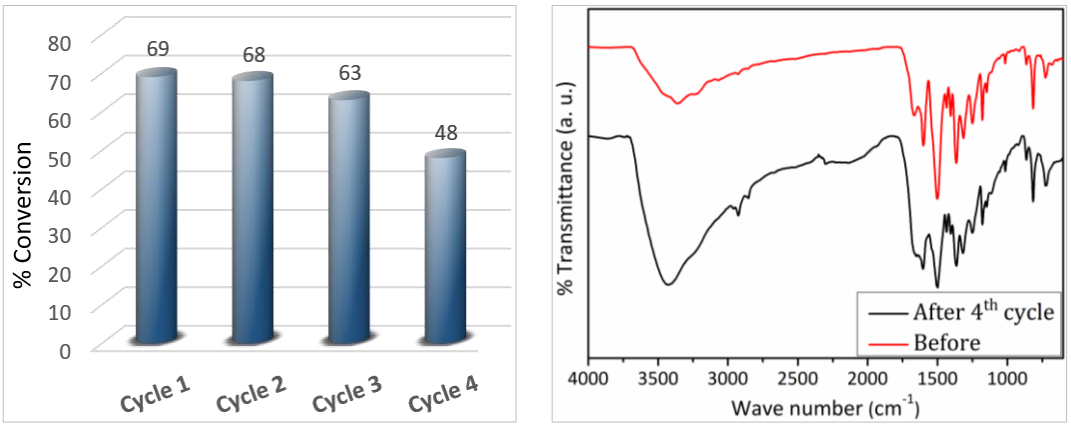

(a) (b)

Figure 3.8 (a) Catalytic conversion and recyclability up to 4th cycle. (b) FT-IR spectra of MOP-Am2 before (red) and after (black) 4th cycle of reactions

3.2.6 Carbon efficiency

Carbon efficiency or the total organic carbon or carbon balance during the catalytic conversion has been examined to substantiate the carbon emission into the environment. The percentage carbon balance or the quantitative emission of carbon to the environment during the aforementioned oxidation of benzyl alcohol is determined by using modified Walkley-Black redox titration method [26]. It is calculated by taking the ratio of the summation of carbon quantities in the detected product including minor/side products and unreacted substances to the initial carbon content in the reactant.

It is determined by digesting as well as oxidizing the reactant side and product side with chromic acid followed by titrating the remaining unreacted acid solution with aqueous $Fe(NH_4)_2(SO_4)_2$ solution. The results are summarized in Tables 3.4 with archetypal substrates.

Table 3.4 Carbon balance or total organic carbon (OC) for the anaerobic oxidation of benzyl alcohol derivatives.

Entry	Weight taken	*Before reaction*		*After reaction*		%OC
		Titrant value of 0.5M Fe $(NH_4)_2(SO_4)_2$ (mL)	OC content quantity on reactant side (mg)	Titrant value of 0.5M Fe $(NH_4)_2(SO_4)_2$ (mL)	OC content quantity on product side after 4 h. (mg)	
20a	30 µL	3.2	23.85	3.5	23.40	98.11
20b	30 mg	3.7	23.10	4.0	22.65	98.05
20c	30 µL	4.7	21.6	5.0	21.15	97.91
20d	30 mg	3.8	22.95	4.0	22.65	98.69
20e	30 mg	2.3	25.20	2.4	25.05	99.40
20f	30 mg	7.1	18.00	7.3	17.7	98.33
20g	45 mg	1.7	26.10	2.0	25.65	98.27
20h	55 mg	3.5	23.4	3.8	22.95	98.07

For the oxidation of benzyl alcohol derivatives, the conversion maintained its percentage carbon balance in the range of ~98–99% (Figure 3.9). Perhaps an unimportant experimental error at the end-point detection is explicable. Thus, no organic carbon emission or loss has been observed at the end of the 4 h reaction in the anaerobic benzyl alcohol oxidation reaction, and its selectivity was maintained.

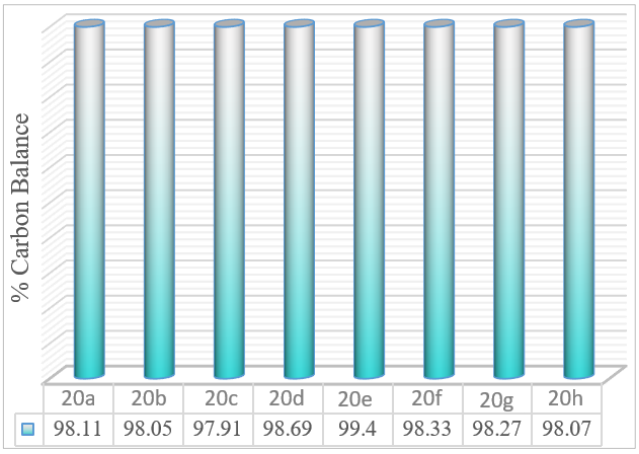

Figure 3.9 Percentage carbon balance in anaerobic oxidation of benzyl alcohol derivatives after 4 h of reaction time

3.3 Summary

In this chapter, the triazine moiety of MOP-Am2 with extended π-cloud is exploited to facilitate the anaerobic oxidation of benzyl alcohols via the intermediate hydride formation. The high electron rich triazine scaffold on the surface interact with the benzylic carbon enhancing the electron density on the LUMO of benzylic C–H. As a result the natural charge on the H-atom enhances while making the C–H bond labile. Computational study as well as the *in-situ* reduction experiments also validated the findings. Moreover, the reported MOP-Am2 is identified as its first kind as metal free organocatalyst promoter to study such oxidant free anaerobic oxidation of benzyl alcohols. Further investigation in the improvement of reaction conversion, affordability, catalyst reusability and industrial applicability will be discussed in the next chapter by taking a similar forefront multicomponent organic transformation reaction.

3.4 Experimental Section

3.4.1 Materials and methods

All chemicals employed in this study are purchased from commercial sources (Sigma Aldrich, Alfa Aesar and Merck) and used as such without further purification until otherwise mentioned. The powder X-ray diffraction (PXRD) patterns are recorded in D8 ADVANCE X-ray using monochromated Cu Kα (λ = 1.542 Å) radiation from Bruker. The UV-Vis diffuse reflectance spectra (UV-Vis DRS) are recorded on a Shimadzu UV-vis spectrophotometer. The reaction progress is monitored by TLC using TLC silica gel F254 250 μm precoated-plates from Merck and the product formation is confirmed by performing GCMS analysis from Perkin Elmer using Turbomass-VER software.

3.4.2 General procedure for oxidation of benzyl alcohols

In a dry Schlenk tube 0.5 mmol of benzyl alcohol derivatives was added to 1 mL of toluene. To this mixture, KOH (2 equiv) and 10% w/w MOP-Am2 with respect to benzyl alcohol derivatives were added. The whole mixture was heated at 85 °C for 4 h. The progress of the reaction was monitored by TLC and quantitative product formation after completion of reaction was analyzed by GC-MS analyzer.

3.4.3 Determination of carbon efficiency

Total organic carbon (OC) or carbon balance during the transformation reactions is measured using modified Walkley and Black method of redox titration where chromic acid is used as digester as well as oxidizing agent and the excess Cr(VI) is titrated against 0.5 M $Fe(NH_4)_2(SO_4)_2$ solution.

The redox reaction involved is-

$$2\ Cr_2O_7^{2-} + 3\ C^0 + 16\ H^+ \quad \leftrightarrow \quad 4\ Cr^{3+} + 3\ CO_2 + 8\ H_2O \qquad \text{------ (v)}$$

Therefore, 1 mL of 1N $K_2Cr_2O_7$ solution = 0.003 g of Carbon.

$$\text{Thus, \% OC} = \frac{(B-S)\times M[Fe(II)]\times 0.003\times 100}{\text{Amount of test sample in g}} \qquad \text{---------- (vi)}$$

Where, B= Titrant volume of blank solution, i.e. without sample

S= Titrant volume for Substrate solution

M[Fe(II)]= Concentration of $Fe(NH_4)_2(SO_4)_2$ solution

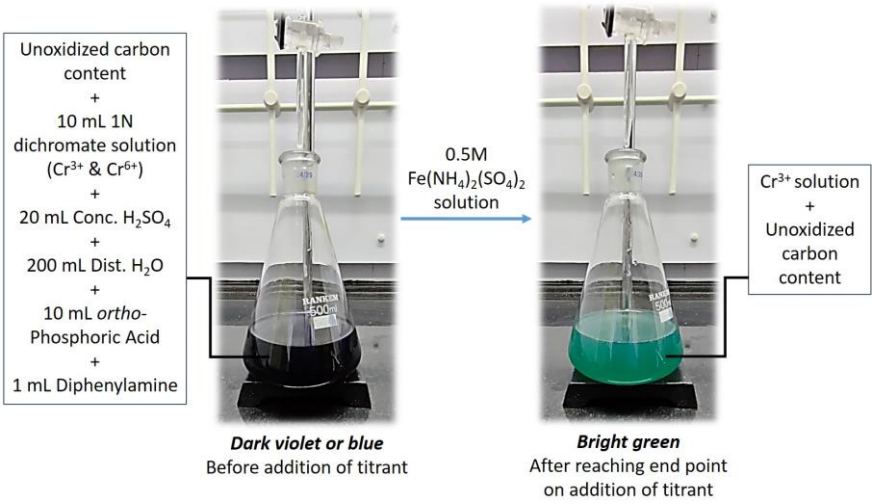

Figure 3.10 Pictorial demonstration of the carbon balance determination using modified Walkley-Black method of redox titration

30 mg of test sample was taken in a 500 mL conical flask. To it 10 mL of 1N $K_2Cr_2O_7$ solution and 20 mL of conc. H_2SO_4 were added. The mixture was heated at 140 °C for 3-4 minute and then it was allowed to digest for half an hour. Once the solution attains the room temperature, 200 mL of distilled water, 10 mL of *ortho*-Phosphoric acid and 1 mL of Diphenylamine indicator are added and swirl steadily to develop a deep violet or blue color solution. Then the mixture is titrated against 0.5M $Fe(NH_4)_2(SO_4)_2$ solution until a bright green color appeared.

3.4.4 DFT computation

The geometric optimization of a basic unit of MOP-Am2 and other substrates in the reactions have been performed in Gaussian16 suite of program [27]. All the structures were optimized without any symmetry constraint at BP86-D3BJ/6-311++G** level of theory [28]. This theory includes pure GGA functional with third order empirical dispersion correction by Grimme employing Becke-Johnson damping function [29]. Harmonic vibrational frequency calculations were also performed which indicates that the structures are real minima on the potential energy surface. Nucleus independent chemical shift (NICS) were also calculated by placing a ghost atom (symbol Bq) at 1Å above the plane of the six membered rings [30]. Non-covalent interaction index were calculated using Multiwfn program code while symmetry adapted perturbation theory (SAPT) were performed using PSI4 program code [31,32].

3.4.5 In-situ reduction of diphenylacetylene

In a 20 mL Schlenk tube 0.5 mmol of 4-methylbenzyl alcohol, 0.25 mmol of diphenylacetylene, KOH (2 equiv. w. r. t. alcohol), 10 wt % of MOP-Am2, 10 mol% of Pd/C (10% Pd/C) w. r. t. diphenylacetylene and 2 mL of toluene were added and heated at 85-90 ℃ for 8 h. The reaction is monitored using TLC. The reaction mixture was purified using column chromatography and characterized by NMR spectroscopy.

3.5 Bibliography

[1] Zhu, J., Wang, P. C., and Lu, M. Selective oxidation of benzyl alcohol under solvent-free condition with gold nanoparticles encapsulated in metal-organic framework. *Applied Catalysis A: General*, 477:125-131, 2014.

[2] Bekhradnia, A. R., Zahir, F., and Arshadi, S. Selective oxidation of organic compounds using pyridinium-1-sulfonate fluorochromate, $C_5H_5NSO_3H[CrO_3F]$ (*PSFC*). *Monatshefte für Chemie-Chemical Monthly*, 139:521-523, 2008.

[3] Rautiainen, S., Simakova, O., Guo, H., Leino, A. R., Kordás, K., Murzin, D., Leskelä, M., and Repo, T. Solvent controlled catalysis: Synthesis of aldehyde, acid or ester by selective oxidation of benzyl alcohol with gold nanoparticles on alumina. *Applied Catalysis A: General*, 485:202-206, 2014.

[4] Della Pina, C., Falletta, E., and Rossi, M. Highly selective oxidation of benzyl alcohol to benzaldehyde catalyzed by bimetallic gold–copper catalyst. *Journal of Catalysis*, 260(2):384-386, 2008.

[5] Corey, E. J. and Suggs, J. W. Pyridinium chlorochromate. an efficient reagent for oxidation of primary and secondary alcohols to carbonyl compounds. *Tetrahedron Letters* 16(31):2647-2650, 1975.

[6] Omura, K., Sharma, A. K., and Swern, D. Dimethyl sulfoxide-trifluoroacetic anhydride. new reagent for oxidation of alcohols to carbonyls. *The Journal of Organic Chemistry,* 41(6):957-962, 1976.

[7] Meyer, S. D. and Schreiber, S. L. Acceleration of the Dess-Martin oxidation by water. *The Journal of Organic Chemistry*, 59(24):7549-7552, 1994.

[8] Choudhary, V. R., Dumbre, D. K., and Bhargava, S. K. Oxidation of benzyl alcohol to benzaldehyde by *tert*-butyl hydroperoxide over nanogold supported on TiO_2 and other transition and rare-earth metal oxides. *Industrial & Engineering Chemistry Research*, 48(21):9471-9478, 2009.

[9] Tareq, S. S., Saiman, M. I., Hin, T. Y. Y., Abdullah, A. H., and Rashid, U. The impact of hydrogen peroxide as an oxidant for solvent-free liquid phase oxidation of benzyl alcohol using Au-Pd supported carbon and titanium catalysts. *Bulletin of Chemical Reaction Engineering & Catalysis*, 13(2):373-385, 2018.

[10] Ryland, B. L., McCann, S. D., Brunold, T. C., and Stahl, S. S. Mechanism of alcohol oxidation mediated by copper(II) and nitroxyl radicals. *Journal of the American Chemical Society*, 136(34):12166-12173, 2014.

[11] Qi, Y., Luan, Y., Peng, X., Yang, M., Hou, J., and Wang, G. Design and synthesis of an Au@MIL-53(NH_2) catalyst for a one-pot aerobic oxidation/Knoevenagel condensation reaction. *European Journal of Inorganic Chemistry*, 2015(30):5099-5105, 2015.

[12] Göksu, H., Burhan, H., Mustafov, S.D. and Şen, F. Oxidation of benzyl alcohol compounds in the presence of carbon hybrid supported platinum nanoparticles (Pt@CHs) in oxygen atmosphere. *Scientific Reports*, 10(1):5439, 2020.

[13] Parmeggiani, C., Matassini, C., and Cardona, F. A step forward towards sustainable aerobic alcohol oxidation: new and revised catalysts based on transition metals on solid supports. *Green Chemistry*, 19(9):2030-2050, 2017.

[14] Peng, L., Wu, S., Yang, X., Hu, J., Fu, X., Li, M., Bai, L., Huo, Q., and Guan, J. Oxidation of benzyl alcohol over metal organic frameworks M-BTC (M= Co, Cu, Fe). *New Journal of Chemistry*, 41(8):2891-2894, 2017.

[15] Isaka, Y., Kondo, Y., Kuwahara, Y., Mori, K., and Yamashita, H. Incorporation of a Ru complex into an amine-functionalized metal-organic framework for enhanced activity in photocatalytic aerobic benzyl alcohol oxidation. *Catalysis Science & Technology*, 9(6):1511-1517, 2019.

[16] Liu, J., Yu, H., Wang, L., Deng, Z., and Vatsadze, S. Z. In-situ preparation of palladium nanoparticles loaded ferrocene based metal-organic framework and its application in oxidation of benzyl alcohol. *Journal of Molecular Structure*, 1198:126895, 2019.

[17] Li, Z., Zhang, J., Jing, X., Dong, J., Liu, H., Lv, H., Chi, Y., and Hu, C. A polyoxometalate@covalent triazine framework as a robust electrocatalyst for selective benzyl alcohol oxidation coupled with hydrogen production. *Journal of Materials Chemistry A*, 9(10):6152-6159, 2021.

[18] Xu, C., Qian, L., Lin, J., Guo, Z., Yan, D., and Zhan, H. Heptazine-based porous polymer for selective CO_2 sorption and visible light photocatalytic oxidation of benzyl alcohol. *Microporous and Mesoporous Materials*, 282:9-14, 2019.

[19] Wei, G., Wang, L., Ding, Z., Yuan, R., Long, J., and Xu, C. Carbazole-involved conjugated microporous polymer hollow spheres for selective photocatalytic oxidation of benzyl alcohol under visible-light irradiation. *Journal of Colloid and Interface Science*, 642:648-657, 2023.

[20] Lin, C. Y., Zhang, D., Zhao, Z., and Xia, Z. Covalent organic framework electrocatalysts for clean energy conversion. *Advanced Materials*, 30(5):1703646, 2018.

[21] Feng, B., Hou, Z., Wang, X., Hu, Y., Li, H., and Qiao, Y. Selective aerobic oxidation of styrene to benzaldehyde catalyzed by water-soluble palladium (II) complex in water. *Green chemistry*, 11(9):1446-1452, 2009.

[22] Khatioda, R., Talukdar, D., Saikia, B., Bania, K. K., and Sarma, B. Constructing two dimensional amide porous polymer to promote selective oxidation reactions. *Catalysis Science & Technology*, 7(14):3143-3150, 2017.

[23] Xu, J., Zhuang, R., Bao, L., Tang, G., and Zhao, Y. KOH-mediated transition metal-free synthesis of imines from alcohols and amines. *Green Chemistry*, 14(9):2384-2387, 2012.

[24] Khatioda, R., Pathak, D., and Sarma, B. Cu(II) Complex onto a pyridine-based porous organic polymer as a heterogeneous catalyst for nitroarene reduction. *ChemistrySelect*, 3(23):6309-6320, 2018.

[25] Gomes, R., Bhanja, P., and Bhaumik, A. A triazine-based covalent organic polymer for efficient CO_2 adsorption. *Chemical Communications*, 51(49):10050-10053, 2015.

[26] Gelman, F., Binstock, R., and Halicz, L. Application of the Walkley–Black titration for the organic carbon quantification in organic rich sedimentary rocks. *Fuel*, 96:608-610, 2012.

[27] Frisch, M. J., Trucks, G. W., Schlegel, H. B., Scuseria, G. E., Robb, M. A., Cheeseman, J. R., Scalmani, G., Barone, V., Petersson, G. A., Nakatsuji, H., and Li, X. Gaussian 16, Revision A.03, Gaussian, Inc., Wallingford CT. 2016.

[28] Becke, A. D. Density-functional exchange-energy approximation with correct asymptotic behavior. *Physical Review A*, 38(6):3098, 1988.

[29] Becke, A. D. and Johnson, E. R. A density-functional model of the dispersion interaction. *The Journal of Chemical Physics*, 123(15):154101, 2005.

[30] Schleyer, P. V. R., Maerker, C., Dransfeld, A., Jiao, H., and van Eikema Hommes, N. J. Nucleus-independent chemical shifts: a simple and efficient aromaticity probe. *Journal of the American Chemical Society*, 118(26):6317-6318, 1996.

[31] Tian, L., Multiwfn: A Multifunctional Wavefunction Analyzer (version 3.1), 2015. Available from: <http://Multiwfn.codeplex.com> (accessed May 23).

[32] Turney, J. M., Simmonett, A. C., Parrish, R. M., Hohenstein, E. G., Evangelista, F. A., Fermann, J. T., Mintz, B. J., Burns, L. A., Wilke, J. J., Abrams, M. L., and Russ, N. J. Psi4: an open-source ab initio electronic structure program. *Wiley Interdisciplinary Reviews: Computational Molecular Science*, 2(4):556-565, 2012.

3.6 Representative Spectra

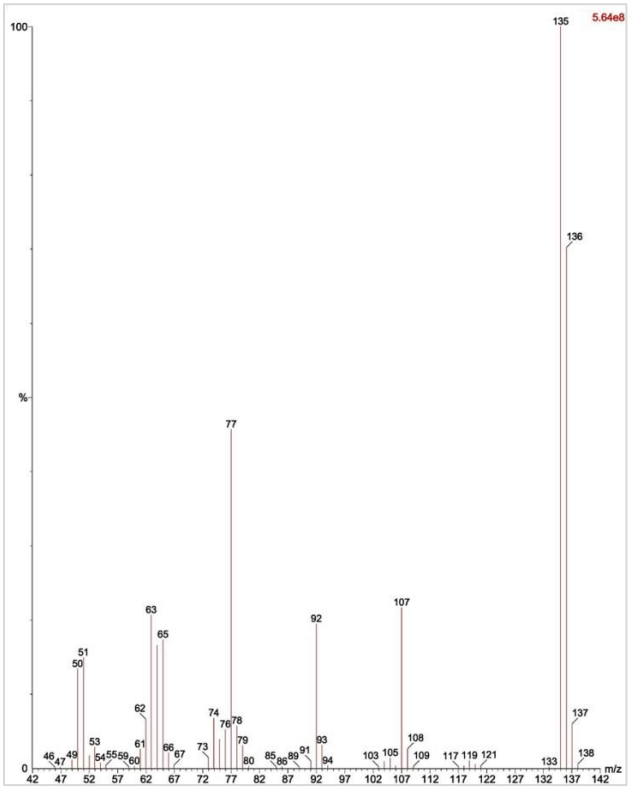

Figure 3.11 Mass spectrum (EI⁺) *m/z* of **20c**

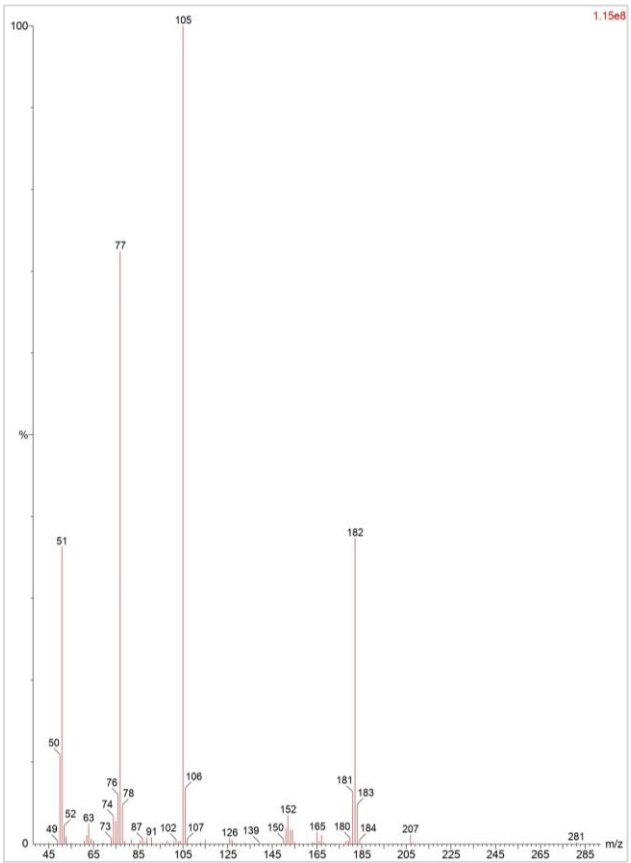

Figure 3.12 Mass spectrum (EI⁺) *m/z* of **20e**

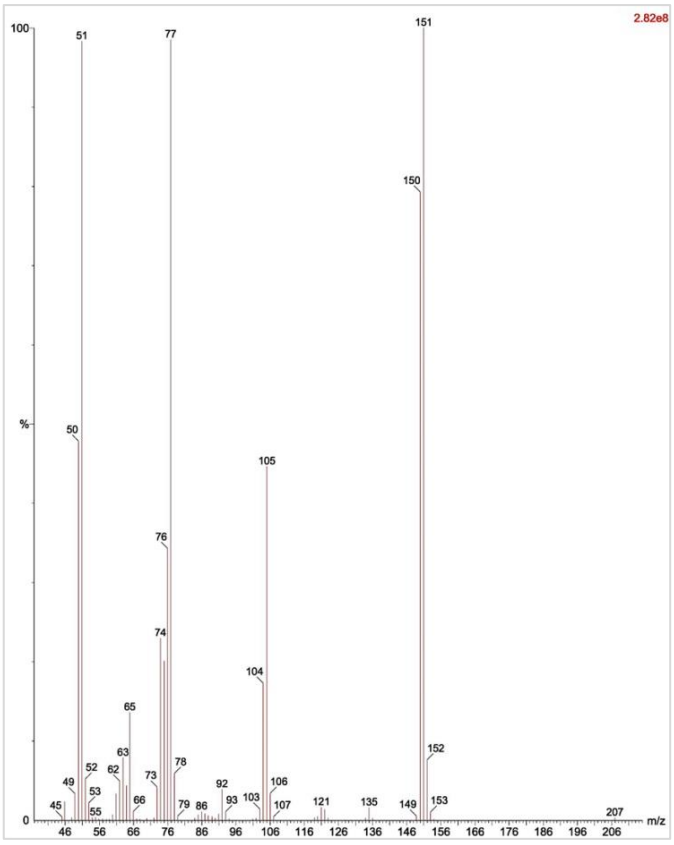

Figure 3.13 Mass spectrum (EI⁺) *m/z* of **20f**

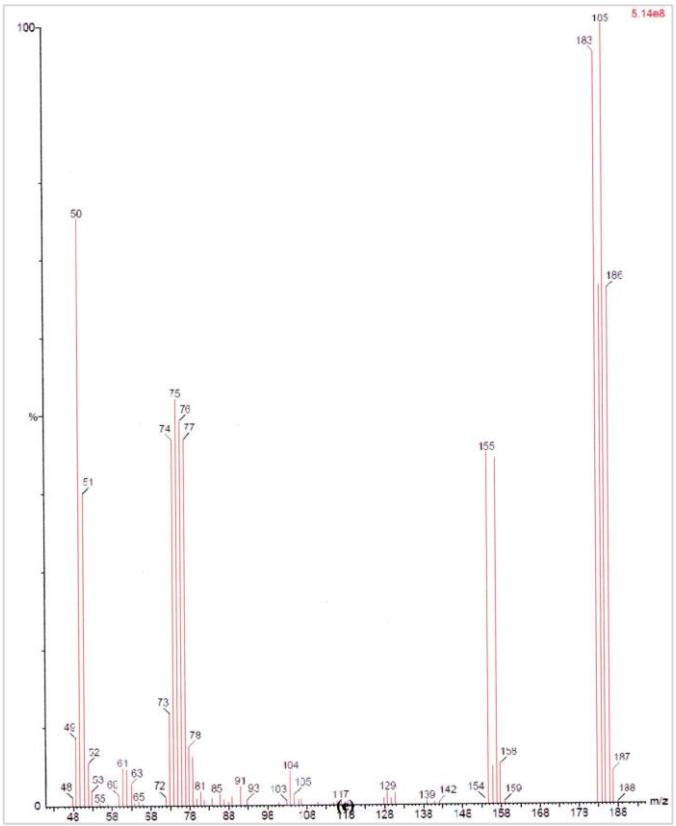

Figure 3.14 Mass spectrum (EI⁺) *m/z* of **20h**